Rubaiy Hussein (Orcid ID: 0000-0002-1489-5576)

Xu Shang-Zhong (Orcid ID: 0000-0002-7295-9347)

T-type Ca^{2+} channel blocker mibefradil blocks ORAI channels via acting on extracellular surface

Pengyun Li[1,2], Hussein N Rubaiy[1], Gui-Lan Chen[1,2], Thomas Hallett[1], Nawel Zaibi[1], Bo Zeng[2], Rahul Saurabh[1], Shang-Zhong Xu[1]*

[1]Centre for Atherothrombosis and Metabolic Disease, Hull York Medical School, University of Hull, Hull, HU6 7RX, UK

[2]Key Laboratory of Medical Electrophysiology, Ministry of Education, and Institute of Cardiovascular Research, Southwest Medical University, Luzhou, 646000, China.

* To whom correspondence should be addressed:

Dr. S.Z. Xu, Hull York Medical School, University of Hull, Hull, HU6 7RX, United Kingdom. Tel: + (44) 1482 465372; Fax: + (44) 1482 465390; e-mail: sam.xu@hyms.ac.uk

Short title: Mibefradil inhibits ORAI channels

Abstract

BACKGROUND AND PURPOSE Mibefradil (Mib), a T-type Ca^{2+} channel blocker, has been investigated for treating solid tumours. However, its underlying mechanisms are still unclear. Here we aimed to investigate the pharmacological aspect of Mib on ORAI store-operated Ca^{2+} channels.

EXPERIMENTAL APPROACH Human ORAI1-3 in tetracycline-regulated pcDNA4/TO vectors was transfected into HEK293 T-REx cells with STIM1 stable expression. The ORAI currents were recorded by whole-cell and excised-membrane patch clamp. Ca^{2+} influx or release was measured by Fura-PE3/AM. Cell growth and death were monitored by WST-1, LDH assays and flow cytometry.

KEY RESULTS Mib inhibited ORAI1, ORAI2 and ORAI3 currents in a dose-dependent manner. The IC_{50} for ORAI1, ORAI2 and ORAI3 was 52.6 µM, 14.1 µM and 3.8 µM, respectively. Outside-out patch demonstrated that perfusion of 10 µM Mib to the extracellular surface completely blocked ORAI3 currents and single channel activity evoked by 2-APB. Intracellular application of Mib did not alter ORAI3 channel activity. Mib at higher concentrations (>50 µM) inhibited Ca^{2+} release, but had no effect on cytosolic STIM1 translocation evoked by thapsigargin. The inhibition of Mib on ORAI channels is structure-related, since other T-type Ca^{2+} channel blockers with different structures, such as ethosuximide and ML218, had no or very small effect on ORAI channels. Moreover, Mib inhibited cell proliferation, induced apoptosis and arrested cell cycle progression.

CONCLUSIONS AND IMPLICATIONS Our results suggest that Mib is a potent extracellular ORAI channel blocker, which provides a new pharmacological profile for the compound in regulating cell growth and death as an anti-cancer drug.

ORAI channels	TRPM3
G protein-coupled receptors	TRPV1
voltage-gated calcium channel	TRPA1
KV10.1 channel	L-type VGCC
ATP-activated K^+ channels	
two P domain potassium channels	Design & Analysis
Ca^{2+}-activated Cl^- channel	
TRPM7	

Abbreviations

2-APB, 2-aminoethoxydiphenyl borate; CFP, cyan fluorescent protein; CRAC, Ca^{2+}-release activated Ca^{2+} channels; DMSO, dimethyl sulphoxide; ER, endoplasmic reticulum; ESM, ethosuximide; EYFP, enhanced yellow fluorescent protein; FCS, fetal calf serum; HAEC, human aortic endothelial cells; IP$_3$R, GPCR, G protein-coupled receptors; inositol trisphosphate receptor; *IV,* current-voltage; LDH, lactate dehydrogenase; Mib, mibefradil; PTK, protein tyrosine kinase; SERCA, sarco (endo)plasmic reticulum Ca^{2+}-ATPase; SOCE, store-operated Ca^{2+} entry; STIM1, stromal interaction molecule 1; TEA, tetraethylammonium; Tet, tetracycline; TIRF, total internal reflection fluorescence; TG, thapsigargin; TRP, transient receptor potential; TRPC, transient receptor potential canonical; VGCC, voltage gated calcium channel

Bullet point summary

What is already known

- Mibefradil is a T-type channel blocker and has been repurposed as an anti-cancer drug.
- ORAI proteins are store-operated Ca^{2+} channel molecules and can regulate cell growth and death.

What this study adds

- We discovered that mibefradil can inhibit ORAI channels.
- The action mode via extracellular surface and the regulation of proliferation and apoptosis.

Clinical significance

- This finding gives a new pharmacological mechanism for the classic T-type channel blocker.
- Inhibition on ORAI channels and store-operated Ca^{2+} entry could explain its anti-cancer action.

Introduction

ORAI channels have been regarded as the molecular fingerprints of Ca^{2+}-release activated Ca^{2+} (CRAC) channels, the highly Ca^{2+} selective store–operated channels (SOCs) (Feske et al., 2006; Prakriya et al., 2006). The channels can be activated by the depletion of endoplasmic reticulum (ER) Ca^{2+} stores via the activation of G protein-coupled receptors (GPCR) and/or protein tyrosine kinase (PTK) coupled receptors. ORAI channels are widely expressed in many cell types and highly expressed in vascular smooth muscle cells (Trebak, 2012) and proximal tubular cells (Zeng et al., 2017). There are three isoforms of ORAI channels, i.e., ORAI1-3. Loss-of-function mutation of ORAI1 caused immune deficiency (Feske et al., 2006) and dysfunction of thrombus formation (Bergmeier et al., 2009; Braun et al., 2009). Inhibition on ORAI channels enhances diabetic proteinuria (Zeng et al., 2017). Therefore, these channels may act as potential therapeutic targets for immune disorders, cardiovascular diseases and diabetic complications.

Mibefradil (Mib), also known as Ro 40-5967 (Bezprozvanny & Tsien, 1995), is a tetralol derivative chemically distinct from other calcium channel antagonist. It has been reported as a potent T-type voltage-gated calcium channel (VGCC) blocker with a high selectivity over L-type VGCC (10- to 15-fold preference for T-type over L-type) (Martin et al., 2000; Mishra & Hermsmeyer, 1994). It blocks all three subtypes of T-type channel, i.e., $Ca_v3.1$, $Ca_v3.2$, and $Ca_v3.3$, with an IC_{50} of 5.8-7.2 µM (Alexander et al., 2017). Mib was initially developed as a cardiovascular drug and used in clinic with the trade name Posicor® to treat hypertension and angina (Lee et al., 2002), but withdrawn from the market by Hoffmann-La Roche in 1998 because of drug interactions with liver enzymes (SoRelle, 1998). Recently, Mib has been repurposed from an abandoned antihypertensive to a targeted solid tumour treatment, and it has been rescued from drug-drug interactions by using short-term dose exposure (Holdhoff et al., 2017). Mib is currently in a phase Ib clinical trial with the National Cancer Institute Adult Brain Tumour Consortium (Holdhoff et al., 2017). The mechanism of anti-cancer therapy was speculated via the blockage of Ca^{2+} influx through T-type channels, but it is still unclear how the T-type channel in non-excitable cancer cells can be activated and thus exerted its anti-tumour effects.

Since ORAI channels are regulated by GPCR via many hormones and growth factors and VGCC may have a functional interaction with ORAI/STIM1 (Wang et al., 2010), and additionally Ca^{2+} influx via store-operated channels is critical for cell proliferation and

apoptosis (Abdullaev et al., 2008), we therefore hypothesize that the T-type channel blocker Mib may exert its effect beyond acting on T-type channels. Here we examined the effect of Mib on ORAI channels using inducible HEK293 T-REx cells overexpressed with ORAIs and STIM1, and found that Mib had a potent inhibition on ORAI channels.

Methods

Cell culture and transfection

Human ORAIs (GenBank accession number: ORAI1, NM_032790; ORAI2, NM_032831; ORAI3, NM_152288) in pcDNA4/TO tetracycline-regulatory vector tagged with fluorescent report genes (mCherry-ORAI1, mCherry-ORAI2 and monomeric cyan fluorescent protein mCFP)-ORAI3 were transfected into HEK-293 T-REx cells (RRID: CVCL_D585, Invitrogen, UK). The human STIM1 (accession number: NM_001277961) tagged with enhanced yellow fluorescent protein at the C-terminus (STIM1-EYFP) was stably co-expressed in the cells with ORAIs. The detail procedures for transfection were described previously (Zeng et al., 2012). The cells with stable expression of STIM1-EYFP and inducible ORAIs were used in the study. The functional expression of ORAIs and STIM1 in the transfected cells have been characterized in our previous reports (Daskoulidou et al., 2015; Zeng et al., 2014; Zeng et al., 2017). The cells were seeded onto coverslips in culture dishes and the ORAI channel expression was induced by 1 $\mu g \cdot mL^{-1}$ tetracycline for 24-72 h before electrophysiological recording or Ca^{2+} imaging. The non-induced cells without addition of tetracycline or non-transfected HEK-293 T-REx cells were used as controls. HEK-293 T-REx cells were grown in DMEM-F12 medium (Invitrogen, UK) containing 10% fetal calf serum (FCS), 100 units·mL^{-1} penicillin and 100 $\mu g \cdot mL^{-1}$ streptomycin. Cells were maintained at 37°C under 95% air and 5% CO_2 and seeded on coverslips prior to experiments. Human aortic endothelial cells (HAECs) were purchased from PromoCell (Heidelberg, Germany), and endothelial cells EA.hy926, a permanent cell line derived from HUVECs, were purchased from American Type Culture Collection (ATCC) (ATCC Cat# CRL-2922, RRID: CVCL_3901) (Middlesex, UK). Endothelial cells were cultured in endothelial cell medium (PromoCell, Germany) supplemented with 2 % FCS, 0.1 ng/ml recombinant human epidermal growth factor, and 1 ng·mL^{-1} basic fibroblast growth factor. HAECs at passages 2–3 were used for the experiment. The human proximal tubular cell line (HK-2) was purchased from LGC standards (ATCC Cat# CRL-2190, RRID: CVCL_0302, UK). HK-2 cells were maintained in DMEM/F-12 medium with 5 mM glucose and

supplemented with 10% FCS, 10 mM HEPES and antibiotics. All the cultured cells were maintained at 37 °C under 95 % air and 5 % CO_2.

Electrophysiology

The procedure for whole-cell clamp is similar to our previous reports (Xu et al., 2012; Zeng et al., 2014; Zeng et al., 2017). Briefly, electrical signal was amplified with an Axopatch 200B patch clamp amplifier and controlled with pClamp software 10. A 1-s ramp voltage protocol from −100 mV to +100 mV was applied at a frequency of 0.2 Hz from a holding potential of 0 mV. Signals were sampled at 3 kHz and filtered at 1 kHz. The glass microelectrode with a resistance of 3-5 MΩ was used. The pipette solution contained (in mM) 145 Cs-methanesulfonate, 10 BAPTA, 8 $MgCl_2$, and 10 HEPES (pH 7.2 adjusted with CsOH). Same pipette solution was used for outside-out patches. The standard bath solution contained (mM): 130 NaCl, 5 KCl, 8 D-glucose, 10 HEPES, 1.2 $MgCl_2$, and 1.5 $CaCl_2$. The pH was adjusted to 7.4 with NaOH. Some experiment was performed using divalent cation free solutions (mM): 150 NaCl, 10 HEPES, 10 D-glucose, 10 EDTA, and 10 tetraethylammonium chloride (TEA-Cl). For single channel recordings, the current was sampled at 10 kHz. The experiment was performed at room temperature (25 °C).

Ca^{2+} measurement and live cell imaging

Cells were preincubated with 2 µM Fura-PE3/AM at 37°C for 30 min in Ca^{2+}-free bath solution (mM):130 NaCl, 5 KCl, 1.2 $MgCl_2$, 10 HEPES, 8 D-glucose, and 0.4 EGTA, followed by a 20-min wash period in the standard bath solution at room temperature. The ratio of Ca^{2+} dye fluorescence (F_{340}/F_{380}) was measured using FlexStation 3 (Molecular Device, USA). Control groups were set in parallel in the 96-well plate. For STIM1 translocation experiment, the procedure was similar to our previous report (Zeng et al., 2012). The stably transfected STIM1-EYFP cells were seeded on 13-mm glass coverslips and cultured for 24 - 48 h. Live cell images for EYFP fluorescence were captured using the microscope equipped with a Nikon Plan Fluor ×100/1.30 oil objective. Total internal reflection fluorescence (TIRF) microscopy was performed in some experiments using a Nikon CFI Apochromat TIRF objective (× 100, 1.49 NA) and sCMOS camera (ORCA-Flash4.0 V2, Hamamatsu, Japan) as we describe previously (Zeng et al., 2017).

Colocalization analysis was performed with NIS-Elements AR v4.30 (Nikon). The images were analyzed with the NIS-Elements software (Version 3.2, Nikon, Tokyo, Japan). All the experiments were performed at room temperature.

Cell proliferation and cell death assays

Cell proliferation was determined using a water-soluble tetrazolium-1 (WST-1) assay in which tetrazolium salts are cleaved by mitochondrial dehydrogenase to form formazan in viable cells. For necrotic cell death, the activity of lactate dehydrogenase (LDH) in the culture medium that released from the cytosol was determined using a Cytotoxicity Detection Kit. The procedures for WST-1 and LDH assays are similar to our previous report (Xu et al., 2008). The absorbance for WST-1 assay and LDH assay were measured using a spectrophotometer.

Fluorescence activated cell sorting (FACS)

The HK-2 cells were seeded in a 6-cm petri dish at a confluence of 5000 cells/mL and incubated in a humidified atmosphere of 5% CO_2 and 95% air at 37 °C for 24 hours. The cells were the pre-treated with different concentrations of Mib for 24-hour incubation, then trypsinised with 0.25% trypsin-EDTA and centrifuged twice for washout with PBS in FACS tubes at 300 g for 5 minutes. The propidium iodide (10 μg/mL) was added to all the tubes and incubated for 15 minutes before mounting for FACS detection. The cell cycle was analysed using CellQuest software.

Chemicals and reagents

All general salts and reagents were from Sigma (UK). Mibefradil dihydrochloride hydrate, 2-aminoethoxydiphenyl borate (2-APB), tetracycline, thapsigargin, ethosuximide and WST-1 and LDH assay kits were purchased from Sigma-Aldrich. ML218 was purchased from Alomone Labs (Jerusalem, Israel). Fura-PE3/AM was purchased from Invitrogen (UK). Fura-

PE3/AM (1 mM) and 2-APB (100 mM) were made up as stock solutions in 100% dimethyl sulphoxide (DMSO). Mib was prepared as 10 mM stock solution in H_2O.

Statistics

Data and statistical analysis comply with the recommendations on experimental design and analysis in pharmacology (Curtis et al., 2015). Data are expressed as mean ± SEM. In this study, *"n"* refers to independent experiments where recombinant channel expression was induced by the addition of tetracycline for 24-72 h to cells maintained on separate coverslips. We consider electrophysiological recordings derived from these separate dishes to constitute independent experiments, as is typical in ion channel experiments. The experiments are not blinded and randomized, but controlled studies. Experimenter treated the cells with tetracycline to induce gene expression as a positive transfected group, and cells without treatment as a negative control. Self-controlled design was used to test drug effect through comparison of before and after drug applications. The unblinded experimental data were analysed in an identical manner for all conditions to eliminate possible operator bias. Mean data were compared using paired *t* test for the results before and after treatment without blinding experimental design, or the ANOVA Bonferroni's post-hoc analysis for comparing more than two groups with significance indicated if *P*<0.05. For all ANOVAs, post hoc tests were only applied when F achieved and there was no significant variance inhomogeneity.

Nomenclature of targets and ligands

Key protein targets and ligands in this article are hyperlinked to corresponding entries in http://www.guidetopharmacology.org, the common portal for data from the IUPHAR/BPS Guide to PHARMACOLOGY (Harding et al., 2018), and are permanently archived in the Concise Guide to PHARMACOLOGY 2017/18 (Alexander et al., 2017).

Results

ORAI channels inhibited by Mib

The expression of human ORAI1-3 tagged with mCherry or CFP and STIM1-EYFP in HEK-293 T-REx cells was induced by tetracycline and confirmed by their plasma membrane localization as described previously (Daskoulidou et al., 2015; Zeng et al., 2017; Zeng et al., 2012). The whole cell current was recorded by patch clamp after 24-72 hours induction of gene expression. The currents of ORAI1 and ORAI2 were activated by thapsigargin (TG, 1 µM) with an inwardly rectifying *IV* curve (Figure 1), which is similar to our previous reports (Zeng et al., 2014; Zeng et al., 2017). The TG-evoked currents achieved maximum within ~5 min after the formation of whole-cell patch configuration (Figure 1A-B). Mib inhibited ORAI1 and ORAI2 currents in a concentration dependent manner with an IC_{50} of 52.6 µM and 14.1 µM, respectively (Figure 1C). For ORAI3 channels, 2-APB (100 µM) was used as a channel activator and the IC_{50} of Mib was 3.8 µM (Figure 1D-E), suggesting that Mib is more potent for ORAI3. In the non-induced HEK-293 T-REx cells, Mib had no significant effect on the endogenous current (Figure 1F).

In order to explore the possibility of class effect due to T-type channel inhibition, the non-selective T-type channel blockers ML218 and ethosuximide (ESM) with different backbone of chemical structures were examined (Figure 2A). ML218 at the concentrations of 1 and 10 µM, which can nearly abolish the T-type channel current (Xiang et al., 2011), had no significant effects on ORAI3 channels (Figure 2B). ESM has an EC_{50} of 0.6 mM for T-type channel (Gomora et al., 2001), but the concentration of ESM at 1 mM only showed a small inhibition (Figure 2C-D), suggesting that both compounds are insensitive to ORAI3 channels. Therefore, the inhibition on ORAI channels by Mib should be chemical structure specific, rather than the indirect class effect of T-type channel inhibition.

Extracellular effects of Mib on ORAI3

The action site for Mib was determined for ORAI3 channel. The higher concentrations of Mib (100 µM) were included in the pipette solution to see whether the activation of ORAI3 current can be prevented. After whole cell configuration was formed for 5 min, 2-APB (100 µM) was added in the bath solution. We found that intracellular application of Mib failed to prevent the ORAI3 current evoked by 2-APB, which could be repeatedly activated by 2-APB after washout (Figure 3A-C), suggesting that the action site of Mib on ORAI3 channel is located in the external surface of the transmembrane domains.

To further confirm their extracellular effects, outside-out patch was performed on the cells overexpressing ORAI3/STIM1. Mib at 10 µM significantly inhibited the ORAI3 current in the outside-out patches (Figure 3D-F).

Single channel activity of ORAI3 was inhibited by Mib

Outside-out membrane patches were performed to explore the effect of Mib on ORAI3 channel activity. Unitary events were detected after perfusion with 2-APB (100 µM) in the Tet-induced ORAI3-STIM1 cells. An example time series plot for single channel open probability was dramatically increased by 2-APB (Figure 4A). The slope conductance for ORAI3 channel evoked by 2-APB was calculated based on the average single channel current amplitude at each voltage step and the value was 71.0 ± 1.4 pS ($n = 11$) (Figure 4B). The amplitude histograms show that the unitary current events of ORAI3 evoked by 2-APB were nearly abolished by Mib (Figure 4C), suggesting the direct inhibition of Mib on ORAI3 channels.

No effect of Mib on STIM1 translocation

The cytosolic STIM1 clustering and movement onto subplasma membrane is a critical process for ORAI and STIM1 interaction and ORAI channel opening, which can act as a new target for ORAI channel modulators (Zeng et al., 2014; Zeng et al., 2012). Therefore we examined the effect of Mib on STIM1 movement. The subplasmalemmal translocation and clustering of STIM1 was induced by ER Ca^{2+} store depletion with thapsigargin (TG) in the HEK293 cells stably expressing STIM1 tagged with EYFP and determined by a TIRF microscopy in comparison to epi-fluorescence images. Pre-treatment with Mib did not affect STIM1-EYFP clustering, cytosolic translocation, and co-localization with ORAI channels near subplasmalemmal membrane (Figure 5, also see Supporting Information Figure 1), suggesting that Mib did not affect the STIM1 clustering and translocation in the cells.

Effects of Mib on ER Ca^{2+} release and SOCE

The effects of Mib on Ca^{2+} release were examined in the EA.hy926 cells, HK-2 cells and HEK-293 T-REx cells. The TG-induced ER Ca^{2+} release was significantly inhibited by high concentrations of Mib (100 µM) in EA.hy926 cells and HK-2 cells (Figure 6A-D). Similar inhibitory effect on Ca^{2+} release was seen in HEK-293 T-REx cells; however, lower concentrations of Mib (0.1-10 µM) had no significant effect on Ca^{2+} release, and there were

no significant effects on basal intracellular Ca^{2+} level (Figure 6E-F). The inhibitory effect of Mib on ER Ca^{2+} release seemed to be unrelated to the ORAI channels, because transfection of ORAI siRNAs significantly reduced the SOCE, but had no influence on ER Ca^{2+} release (Figure 6G-H). Similar siRNA result was observed in the HK-2 cells as we described previously (Zeng et al., 2017). These results suggest that other underlying mechanisms could be involved in the inhibition of ER Ca^{2+} release by Mib. As expected, Mib nearly abolished the SOCE in both EA.hy926 cells and HK-2 cells (Figure 6A-D).

Effect of Mib on cell proliferation and cell death

Anti-tumour effect has been demonstrated for Mib (Haverstick et al., 2000; Santoni et al., 2012) therefore we tested the effects of Mib on cell proliferation and cell death using *in vitro* cell models. Mib significantly inhibited the proliferation of immortalized cell line (HK-2 and EA.hy926 cells) and the primary cultured normal human aortic endothelial cells (HAEC). The EC_{50} of anti-proliferation for HK-2, EA.hy926, and HAEC were 28.2 µM, 5.9 µM, and 14.2 µM, respectively (Figure 7A-B), suggesting that the inhibition of proliferation in endothelial cells is more sensitive to Mib than that in HK-2 cells, which could be due to higher expression level of ORAIs in endothelial cells (Supporting Information Figure 2). Mib also significantly induced cell death as assayed by LDH release (Figure 7C). The effect of Mib on cell cycle was examined using flow cytometry. Lower concentrations of Mib (1, 5 µM) increased the percentage of cells at G0/G1, but at high concentrations decreased the percentage of cells at S phase and G2/M phase (Figure 7D-G).

Discussion

In this study we have found that ORAI channels are blocked by Mib. The blocking effect is concentration-dependent and reversible. The action site is located on the extracellular cell surface. High concentrations of Mib not only reduce SOCE but also inhibit Ca^{2+} release from ER. Mib significantly inhibits cell proliferation and promotes cell apoptosis by arresting the progression of cell cycle from G1/G0 to S phase, and to G2/M phase. These findings provide a new pharmacological profile for Mib, which is commonly used as T-type Ca^{2+} channel blocker and has recently been repurposed as an anti-cancer drug.

ORAI channels are main components of SOCE in the endothelial cells and HK-2 cells, which has been demonstrated by gene silencing using ORAI siRNAs in this study and our previous report (Zeng et al., 2017). Mib at high concentrations nearly abolish the SOCE in the two cell types. The effect on ORAI subtypes has been compared using an inducible overexpressing system, and Mib is more sensitive to ORAI3 than ORAI1 and ORAI2. The EC_{50} for ORAI channel blockage is similar to the EC_{50} for blocking T-type Ca^{2+} channels (Alexander et al., 2017), suggesting the inhibition on SOCE is one of the main mechanisms of action for the compound. Mib seems to be more sensitive to the overexpressed T-type Ca^{2+} channels than the native T-type Ca^{2+} channels, such as T channel isoforms α1G, α1H, and α1I isoforms with an EC_{50} around 1 µM (Martin et al., 2000). Since inhibition of SOCE or ORAI channels has been demonstrated as anti-proliferative in several types of normal and cancer cells (Konig et al., 2013; Umemura et al., 2014; Vaeth et al., 2017), the anti-cancer effect of Mib could be explained at least in part due to the blockage of ORAI channels, rather than the sole blockage on T-type Ca^{2+} channel, although the T-type channels are highly expressed in some types of cancer and have been regarded as the potential therapeutic target for regulating cancer cell growth and death (Zhang et al., 2017).

We have explored the action site of Mib using outside-out patch and whole cell patch with intracellular drug application. Mib inhibits the ORAI3 current and abolishes the single channel open probability extracellularly, suggesting that ORAI channel shows a druggable target on the external surface. The slope conductance of 2-APB-activated ORAI3 channel with 71 pS in this study is much bigger than the chord conductance estimated at a holding potential of -100 mV by noise analysis method in divalent-free solution (Yamashita & Prakriya, 2014). This discrepancy could be due to the differences of bath solution and/or 2-APB concentration. However, direct single channel event detection using step voltage protocol in this study is much more clear and accurate than the noise analysis method. In addition, Mib has no effect on cytosolic STIM1 clustering and movement, suggesting the blockage by Mib is on the channel protein itself. The ER Ca^{2+} release is an initial step for activate ORAI channels or causes SOCE, Mib at lower concentrations (<10 µM) has no significant effect on ER Ca^{2+} release, which is consistent with the report on calcium transient and spontaneous rhythmic calcium oscillations (Lowie et al., 2011); however, the inhibition on Ca^{2+} release by Mib was significant at high concentrations, which could be a mechanism of its cytotoxicity. We have also analysed the basal intracellular Ca^{2+} level and Mib seems to

have no significant effects on the basal Ca^{2+} level in our acute *in vitro* Ca^{2+} detection using Flexstation.

The effect of Mib on cell proliferation and death has been investigated in this study. Mib potently inhibits the proliferation of vascular endothelial cells (human aortic endothelial cells and EA.hy926 cells). This result is accordant with the reports on calf pulmonary artery endothelial cells (Nilius et al., 1997), rat microvascular endothelial cells (Manolopoulos et al., 2000), human pulmonary smooth muscle cells (Rodman et al., 2005) and some cell lines (U87, N1E-115 and COS7) (Panner & Wurster, 2006). ORAI channels are highly expressed in human proximal tubular cells and are involved in the protein reabsorption (Zeng et al., 2017), while T-type Ca^{2+} channel could play a role in calcium reabsorption (Leclerc et al., 2004). We found that high concentrations of Mib (>25 µM) cause apoptosis of proximal tubular cells, suggesting that Mib may impair kidney function. We have also observed the effect of Mib on cell cycle. Mib treatment increases the HK-2 cell number at G0/G1 phase and decreases the cell number in G2/M, suggesting the cell cycle progressing from G1 to S, and G2 to M phase is arrested. This finding is similar to the reports on ovarian cancer cells (Dziegielewska et al., 2016) and Jurkat cells (Huang et al., 2015), which could be related to Ca^{2+} signalling in the initiation of DNA synthesis (G1 to S phase) and the mitosis (G2 to M phase) (Panner & Wurster, 2006). However, high concentrations of Mib (i.e., more than 25 µM) could show non-specific cytotoxicity by stimulating apoptosis and reducing the cell population at G0/G1 phase, since more specific tools to inhibit Ca^{2+} permeable channels, such as siRNAs, mainly increase the cell population at G2/M phase, rather than reduce the cell numbers at G2/M phase (Cai et al., 2009; Zeng et al., 2013). The significant inhibition on Ca^{2+} release by high concentrations of Mib should impair intracellular Ca^{2+} dynamics and thus change cell viability. Several studies have demonstrated the critical roles of ORAIs and STIMs in apoptosis and cancer migration and metastasis (Faouzi et al., 2011; Jardin & Rosado, 2016; Tanwar & Motiani, 2018) and we have shown the potent inhibition on ORAI channels by Mib in this study, for example, the EC_{50} of 3.8 µM for ORAI3, therefore it is reasonable to speculate that the anti-tumour effect of Mib could also be mediated by the inhibition on ORAI channels when high dosage is used for cancer therapy (150-350 mg/day, ClinicalTrials ID: NCT02202993) and the maximum plasma concentration may achieve several micrograms per litre (Holdhoff et al., 2017; Welker et al., 1998).

Apart from the inhibition on ORAI channels, Mib also inhibits K^+ channels, such as KV10.1 channel (Gomez-Lagunas et al., 2017), ATP-activated K^+ channels (Gomora et al., 1999), and two P domain potassium channels (Czirjak & Enyedi, 2006); and Ca^{2+}-activated Cl^- channel (Nilius et al., 1997). It has also been demonstrated to activate TRPM7, but the effective concentration is much higher with an EC_{50} of 53 µM (Schafer et al., 2016). Mib has no effects on TRPM3, TRPV1 and TRPA1, suggesting Mib has some specificity for ion channels. We have also examined other T-channel blockers, such as ML218 and ethosuximide, with different chemical structures. The two compounds have no or small effect on ORAI channels, suggesting the blocking effect of Mib on ORAI channels is specific for its chemical structure, but unrelated to class effect of T-type Ca^{2+} channel blockage.

In conclusion, our data suggest a new pharmacological profile for Mib, which acts as a pan inhibitor for ORAI channels. The specific action site for Mib on ORAI channels is accessible via an extracellular surface, which could be developed as a new target for compound screening or future potential anti-proliferative drug development.

Conflicts of interest

None

Declaration of transparency and scientific rigour

This Declaration acknowledges that this paper adheres to the principles for transparent reporting and scientific rigour of preclinical research as stated in the BJP guidelines for

<u>Design & Analysis</u>, and as recommended by funding agencies, publishers and other organisations engaged with supporting research.

Author Contributions

P.L. performed the cell culture, Ca^{2+} measurement, patch clamp and analysed data. H.N.R. performed the outside-out patch clamp and contributed part of whole cell recording data. G.L.C. performed the patch clamp. T.H. performed Ca^{2+} measurement. N.Z. and R.S. performed the cell growth and death experiments. P.L. and B.Z. performed the STIM1-EYFP movement experiment. S.Z.X initiated the project, generated the ideas and research funds, led the project, interpreted data and wrote the manuscript. All authors commented on the manuscript.

References

Abdullaev IF, Bisaillon JM, Potier M, Gonzalez JC, Motiani RK, & Trebak M (2008). Stim1 and Orai1 mediate CRAC currents and store-operated calcium entry important for endothelial cell proliferation. Circ Res 103**:** 1289-1299.

Alexander SP, Striessnig J, Kelly E, Marrion NV, Peters JA, Faccenda E*, et al.* (2017). THE CONCISE GUIDE TO PHARMACOLOGY 2017/18: Voltage-gated ion channels. Br J Pharmacol 174 Suppl 1**:** S160-S194.

Bergmeier W, Oh-Hora M, McCarl CA, Roden RC, Bray PF, & Feske S (2009). R93W mutation in Orai1 causes impaired calcium influx in platelets. Blood 113**:** 675-678.

Bezprozvanny I, & Tsien RW (1995). Voltage-dependent blockade of diverse types of voltage-gated Ca2+ channels expressed in Xenopus oocytes by the Ca2+ channel antagonist mibefradil (Ro 40-5967). Mol Pharmacol 48**:** 540-549.

Braun A, Varga-Szabo D, Kleinschnitz C, Pleines I, Bender M, Austinat M*, et al.* (2009). Orai1 (CRACM1) is the platelet SOC channel and essential for pathological thrombus formation. Blood 113**:** 2056-2063.

Cai R, Ding X, Zhou K, Shi Y, Ge R, Ren G*, et al.* (2009). Blockade of TRPC6 channels induced G2/M phase arrest and suppressed growth in human gastric cancer cells. Int J Cancer 125**:** 2281-2287.

Curtis MJ, Bond RA, Spina D, Ahluwalia A, Alexander SP, Giembycz MA*, et al.* (2015). Experimental design and analysis and their reporting: new guidance for publication in BJP. Br J Pharmacol 172**:** 3461-3471.

Czirjak G, & Enyedi P (2006). Zinc and mercuric ions distinguish TRESK from the other two-pore-domain K+ channels. Mol Pharmacol 69**:** 1024-1032.

Daskoulidou N, Zeng B, Berglund LM, Jiang H, Chen GL, Kotova O, *et al.* (2015). High glucose enhances store-operated calcium entry by upregulating ORAI/STIM via calcineurin-NFAT signalling. J Mol Med (Berl) 93**:** 511-521.

Dziegielewska B, Casarez EV, Yang WZ, Gray LS, Dziegielewski J, & Slack-Davis JK (2016). T-Type Ca2+ Channel Inhibition Sensitizes Ovarian Cancer to Carboplatin. Mol Cancer Ther 15**:** 460-470.

Faouzi M, Hague F, Potier M, Ahidouch A, Sevestre H, & Ouadid-Ahidouch H (2011). Down-regulation of Orai3 arrests cell-cycle progression and induces apoptosis in breast cancer cells but not in normal breast epithelial cells. J Cell Physiol 226**:** 542-551.

Feske S, Gwack Y, Prakriya M, Srikanth S, Puppel SH, Tanasa B, *et al.* (2006). A mutation in Orai1 causes immune deficiency by abrogating CRAC channel function. Nature 441**:** 179-185.

Gomez-Lagunas F, Carrillo E, Pardo LA, & Stuhmer W (2017). Gating Modulation of the Tumor-Related Kv10.1 Channel by Mibefradil. J Cell Physiol 232**:** 2019-2032.

Gomora JC, Daud AN, Weiergraber M, & Perez-Reyes E (2001). Block of cloned human T-type calcium channels by succinimide antiepileptic drugs. Mol Pharmacol 60**:** 1121-1132.

Gomora JC, Enyeart JA, & Enyeart JJ (1999). Mibefradil potently blocks ATP-activated K(+) channels in adrenal cells. Mol Pharmacol 56**:** 1192-1197.

Harding SD, Sharman JL, Faccenda E, Southan C, Pawson AJ, Ireland S, *et al.* (2018). The IUPHAR/BPS Guide to PHARMACOLOGY in 2018: updates and expansion to encompass the new guide to IMMUNOPHARMACOLOGY. Nucleic Acids Res 46**:** D1091-D1106.

Haverstick DM, Heady TN, Macdonald TL, & Gray LS (2000). Inhibition of human prostate cancer proliferation in vitro and in a mouse model by a compound synthesized to block Ca2+ entry. Cancer Res 60**:** 1002-1008.

Holdhoff M, Ye X, Supko JG, Nabors LB, Desai AS, Walbert T, *et al.* (2017). Timed sequential therapy of the selective T-type calcium channel blocker mibefradil and temozolomide in patients with recurrent high-grade gliomas. Neuro Oncol 19**:** 845-852.

Huang W, Lu C, Wu Y, Ouyang S, & Chen Y (2015). T-type calcium channel antagonists, mibefradil and NNC-55-0396 inhibit cell proliferation and induce cell apoptosis in leukemia cell lines. J Exp Clin Cancer Res 34**:** 54.

Jardin I, & Rosado JA (2016). STIM and calcium channel complexes in cancer. Biochim Biophys Acta 1863**:** 1418-1426.

Konig S, Browne S, Doleschal B, Schernthaner M, Poteser M, Machler H, *et al.* (2013). Inhibition of Orai1-mediated Ca(2+) entry is a key mechanism of the antiproliferative action of sirolimus in human arterial smooth muscle. Am J Physiol Heart Circ Physiol 305**:** H1646-1657.

Leclerc M, Brunette MG, & Couchourel D (2004). Aldosterone enhances renal calcium reabsorption by two types of channels. Kidney Int 66**:** 242-250.

Lee DS, Goodman S, Dean DM, Lenis J, Ma P, Gervais PB*, et al.* (2002). Randomized comparison of T-type versus L-type calcium-channel blockade on exercise duration in stable angina: results of the Posicor Reduction of Ischemia During Exercise (PRIDE) trial. Am Heart J 144**:** 60-67.

Lowie BJ, Wang XY, White EJ, & Huizinga JD (2011). On the origin of rhythmic calcium transients in the ICC-MP of the mouse small intestine. Am J Physiol Gastrointest Liver Physiol 301**:** G835-845.

Manolopoulos VG, Liekens S, Koolwijk P, Voets T, Peters E, Droogmans G*, et al.* (2000). Inhibition of angiogenesis by blockers of volume-regulated anion channels. Gen Pharmacol 34**:** 107-116.

Martin RL, Lee JH, Cribbs LL, Perez-Reyes E, & Hanck DA (2000). Mibefradil block of cloned T-type calcium channels. J Pharmacol Exp Ther 295**:** 302-308.

Mishra SK, & Hermsmeyer K (1994). Selective inhibition of T-type Ca2+ channels by Ro 40-5967. Circ Res 75**:** 144-148.

Nilius B, Prenen J, Kamouchi M, Viana F, Voets T, & Droogmans G (1997). Inhibition by mibefradil, a novel calcium channel antagonist, of Ca(2+)- and volume-activated Cl-channels in macrovascular endothelial cells. Br J Pharmacol 121**:** 547-555.

Panner A, & Wurster RD (2006). T-type calcium channels and tumor proliferation. Cell Calcium 40**:** 253-259.

Prakriya M, Feske S, Gwack Y, Srikanth S, Rao A, & Hogan PG (2006). Orai1 is an essential pore subunit of the CRAC channel. Nature 443**:** 230-233.

Rodman DM, Reese K, Harral J, Fouty B, Wu S, West J*, et al.* (2005). Low-voltage-activated (T-type) calcium channels control proliferation of human pulmonary artery myocytes. Circ Res 96**:** 864-872.

Santoni G, Santoni M, & Nabissi M (2012). Functional role of T-type calcium channels in tumour growth and progression: prospective in cancer therapy. Br J Pharmacol 166**:** 1244-1246.

Schafer S, Ferioli S, Hofmann T, Zierler S, Gudermann T, & Chubanov V (2016). Mibefradil represents a new class of benzimidazole TRPM7 channel agonists. Pflugers Arch 468**:** 623-634.

SoRelle R (1998). Withdrawal of Posicor from market. Circulation 98**:** 831-832.

Tanwar J, & Motiani RK (2018). Role of SOCE architects STIM and Orai proteins in Cell Death. Cell Calcium 69**:** 19-27.

Trebak M (2012). STIM/Orai signalling complexes in vascular smooth muscle. J Physiol 590**:** 4201-4208.

Umemura M, Baljinnyam E, Feske S, De Lorenzo MS, Xie LH, Feng X*, et al.* (2014). Store-operated Ca2+ entry (SOCE) regulates melanoma proliferation and cell migration. PLoS One 9**:** e89292.

Vaeth M, Maus M, Klein-Hessling S, Freinkman E, Yang J, Eckstein M*, et al.* (2017). Store-Operated Ca(2+) Entry Controls Clonal Expansion of T Cells through Metabolic Reprogramming. Immunity 47**:** 664-679 e666.

Wang Y, Deng X, Mancarella S, Hendron E, Eguchi S, Soboloff J*, et al.* (2010). The calcium store sensor, STIM1, reciprocally controls Orai and CaV1.2 channels. Science 330**:** 105-109.

Welker HA, Wiltshire H, & Bullingham R (1998). Clinical pharmacokinetics of mibefradil. Clin Pharmacokinet 35**:** 405-423.

Xiang Z, Thompson AD, Brogan JT, Schulte ML, Melancon BJ, Mi D*, et al.* (2011). The Discovery and Characterization of ML218: A Novel, Centrally Active T-Type Calcium Channel Inhibitor with Robust Effects in STN Neurons and in a Rodent Model of Parkinson's Disease. ACS Chem Neurosci 2**:** 730-742.

Xu SZ, Zeng B, Daskoulidou N, Chen GL, Atkin SL, & Lukhele B (2012). Activation of TRPC cationic channels by mercurial compounds confers the cytotoxicity of mercury exposure. Toxicol Sci 125**:** 56-68.

Xu SZ, Zhong W, Watson NM, Dickerson E, Wake JD, Lindow SW*, et al.* (2008). Fluvastatin reduces oxidative damage in human vascular endothelial cells by upregulating Bcl-2. J Thromb Haemost 6**:** 692-700.

Yamashita M, & Prakriya M (2014). Divergence of Ca(2+) selectivity and equilibrium Ca(2+) blockade in a Ca(2+) release-activated Ca(2+) channel. J Gen Physiol 143**:** 325-343.

Zeng B, Chen GL, Daskoulidou N, & Xu SZ (2014). The ryanodine receptor agonist 4-chloro-3-ethylphenol blocks ORAI store-operated channels. Br J Pharmacol 171**:** 1250-1259.

Zeng B, Chen GL, Garcia-Vaz E, Bhandari S, Daskoulidou N, Berglund LM*, et al.* (2017). ORAI channels are critical for receptor-mediated endocytosis of albumin. Nat Commun 8**:** 1920.

Zeng B, Chen GL, & Xu SZ (2012). Store-independent pathways for cytosolic STIM1 clustering in the regulation of store-operated Ca(2+) influx. Biochem Pharmacol 84**:** 1024-1035.
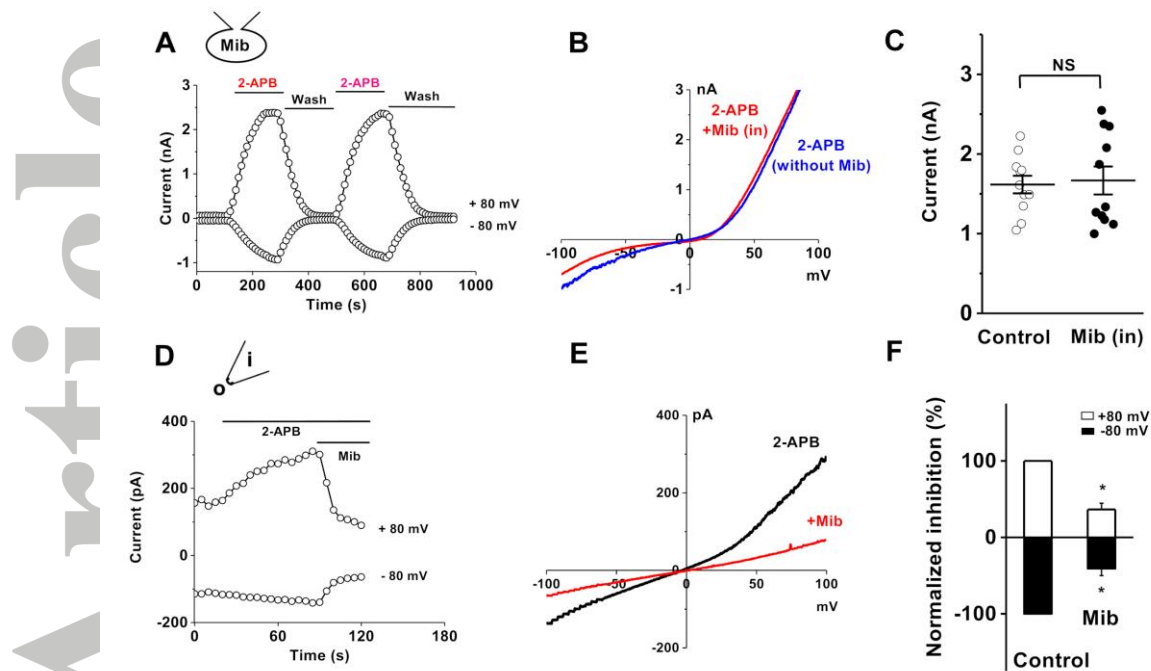
Zeng B, Yuan C, Yang X, Atkin SL, & Xu SZ (2013). TRPC channels and their splice variants are essential for promoting human ovarian cancer cell proliferation and tumorigenesis. Curr Cancer Drug Targets 13**:** 103-116.

Zhang Y, Cruickshanks N, Yuan F, Wang B, Pahuski M, Wulfkuhle J*, et al.* (2017). Targetable T-type Calcium Channels Drive Glioblastoma. Cancer Res 77**:** 3479-3490.
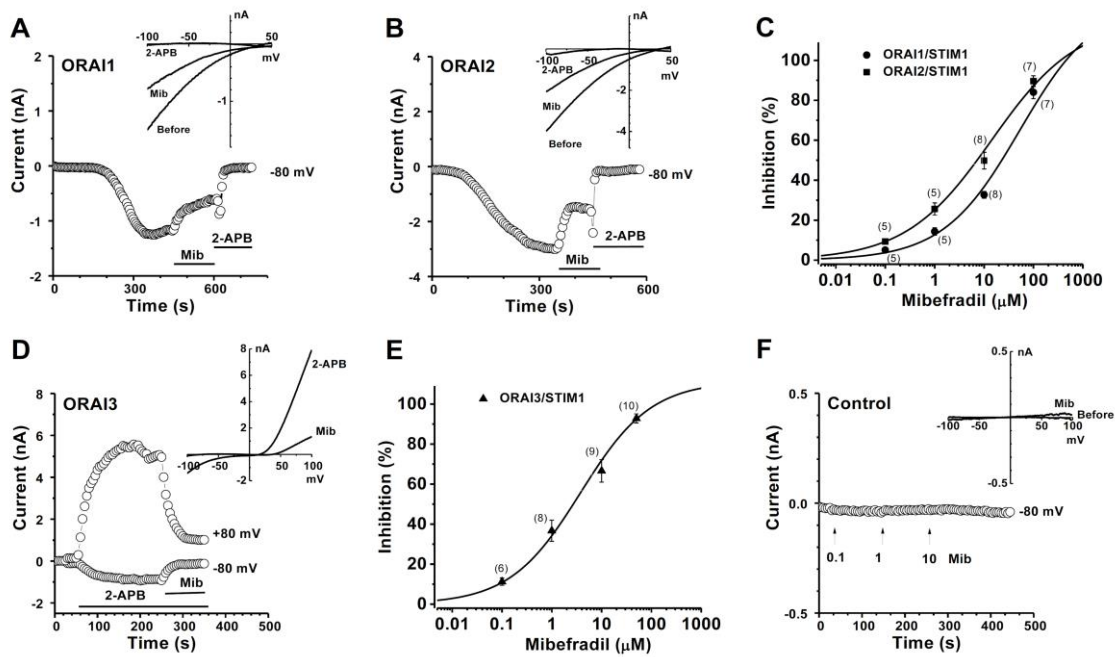
Figure 1 Mibefradil (Mib) inhibits ORAI channels. (A) ORAI1 current in the stable cells overexpressing with mCherry-ORAI1/STIM1-EYFP in the presence of TG (1 µM) in the pipette solution and the effect of Mib (10 µM). (B) ORAI2 current in the cells overexpressing mCherry-ORAI2/STIM1-EYFP in the presence of TG (1 µM) and the effect of Mib (10 µM). (C) Concentration-response curves for Mib on the ORAI1 and ORAI2 with an EC_{50} of 52.6 µM and 14.1 µM, respectively. (D) ORAI3 current in the stable cells overexpressing CFP-ORAI3/STIM1-EYFP was induced by 2-APB (100 µM). Mib (10 µM) inhibited the ORAI3 current. (E) Concentration-response curve for Mib on ORAI3 channel with an EC_{50} of 3.8 µM. (F) Cells without induction of gene expression by tetracycline (Control). The IV curves were shown as insets after leak subtraction. The *n* numbers are shown in the parentheses.

Figure 2 Effect of T-type Ca^{2+} channel blocker ML218 and ethosuximide. (A) Structure of mibefradil, ML218 and ethosuximide (ESM). (B) Effect of ML218 on ORAI3 current. (C) Example of ESM (1 mM) on ORAI3 channel. (D) Normalized data showing the effects of ML218 and ESM on ORAI3 ($n = 5$ for each ML218 treated group; and $n = 5$ for 1 mM ESM-treated group, $^*P < 0.05$).

Figure 3 Extracellular effect of Mib on ORAI3 channels. (A) Whole-cell patch was recorded in the ORAI3 cells using pipette solution containing 100 µM Mib. 2-APB (100 µM) was added in the bath solution. (B) Example *IV* curves for 2-APB-activated ORAI3 current with Mib [Mib (in)] or without Mib (without Mib) in the pipette solution. (C) Mean data for 2-APB activated current recorded with pipette solution containing Mib or without Mib (Control) (*n* = 11 for each group). (D) Example of outside-out patches showing the effect of Mib (10 µM). (E) *IV* curve for outside-out patch in (D). (F) Normalized mean data for the outside-out patch current inhibited by Mib (10 µM) (*n* = 5, *P* < 0.05).
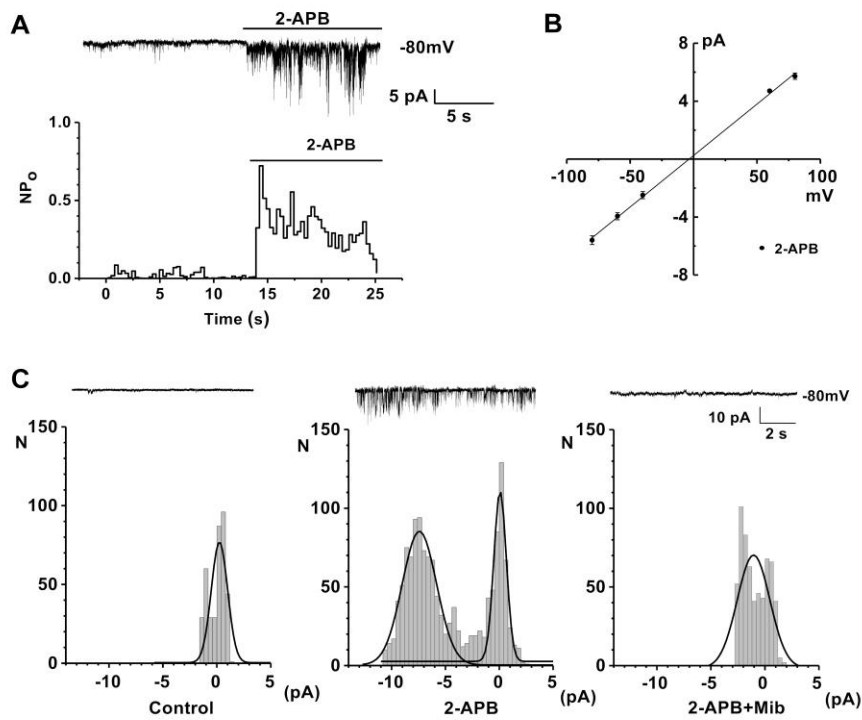
Figure 4 Single channel activity of ORAI3 and the effect of Mib. (A) Original outside-out patch recording showing single channel activity of ORAI3 was induced by 2-APB (100 µM) in Tet-induced ORAI3/STIM1 cells. Time-series plot for single channel open probability (NPo), showing the activation by bath-applied 2-APB. (B) Mean unitary current sizes for 2-APB-evoked single channel events plotted against voltage. The mean slope conductance, fitted by straight lines, was 71.0 ± 1.4 pS ($n = 11$ cells). (C) Example outside-out patch traces and amplitude histograms for control (no 2-APB), 2-APB (100 µM) and 2-APB (100 µM) plus Mib (10 µM) groups.
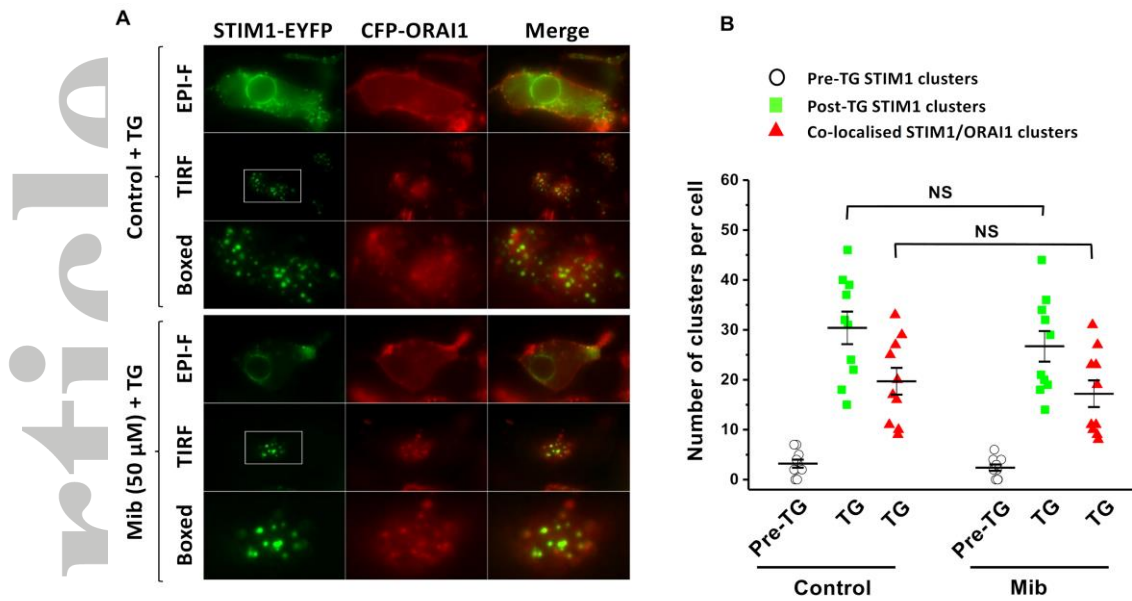
Figure 5 STIM1 subplasmalemmal translocation and STIM1/ORAI1 clustering after Ca^{2+} store depletion in the stable transfected STIM1–EYFP/CFP-ORAI1 cells and the effect of Mib. (A) TG (1 μM) induced STIM1/ORAI1 puncta formation at the plasma membrane. Both TIRF and EPI-F images were sampled and the subplasmalemmal STIM1 clusters (puncta) and co-localization with ORAI1 were analysed. The boxed areas were enlarged in the corresponding panels. (B) Cells pretreated with Mib (50 μM) or without Mib (Control) and then added with TG (1 μM). The data are pooled from 5 independent experiments and ten images for each group were analysed ($n = 10$; NS, non-significant).
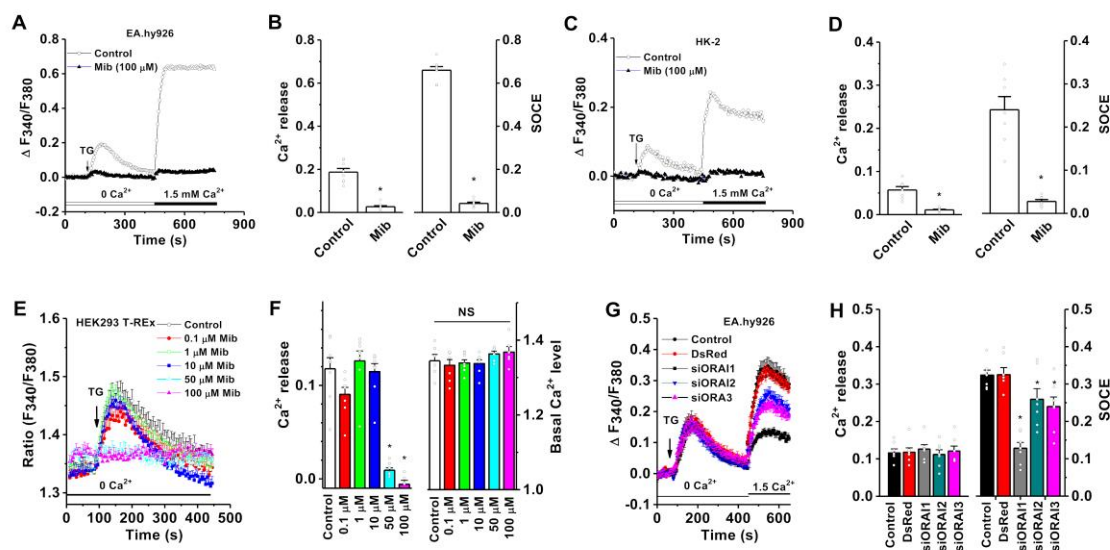
Figure 6 ER Ca^{2+} release and SOCE inhibited by Mib and silencing of SOCE by ORAI siRNAs. (A) Vascular endothelial cells EA.hy926 were loaded with Fura-PE3/AM and the ER Ca^{2+} release was induced by 1 μM thapsigargin (TG). The fluorescence at a ratio of F340/380 was monitored in the group with or without pretreatment with Mib. The SOCE was evoked by refilling 1.5 mM Ca^{2+} in the bath solution. (B) Mean data was measured at the peak of Ca^{2+} release or peak of SOCE ($n = 8$). (C) ER Ca^{2+} release and SOCE in HK-2 cells. (D) Mean data for HK-2 cells ($n = 8$). (E) Effects of Mib at different concentrations on ER Ca^{2+} release in HEK-293 T-REx cells. (F) Mean data for the effect on Ca^{2+} release and basal Ca^{2+} level ($n = 8$). (G) After transfection with ORAI siRNAs (siORAI1, siORAI2 and siORAI3) and the control report fluorescence protein (DsRed) for 48 hours, ER Ca^{2+} release and SOCE were detected by FlexStation 3. (H) Mean ± SEM data for the groups of control (sham transfection); a red fluorescent protein report gene (DsRed); and Orai1-3 siRNAs ($n = 8$ for each group). *$P < 0.05$.
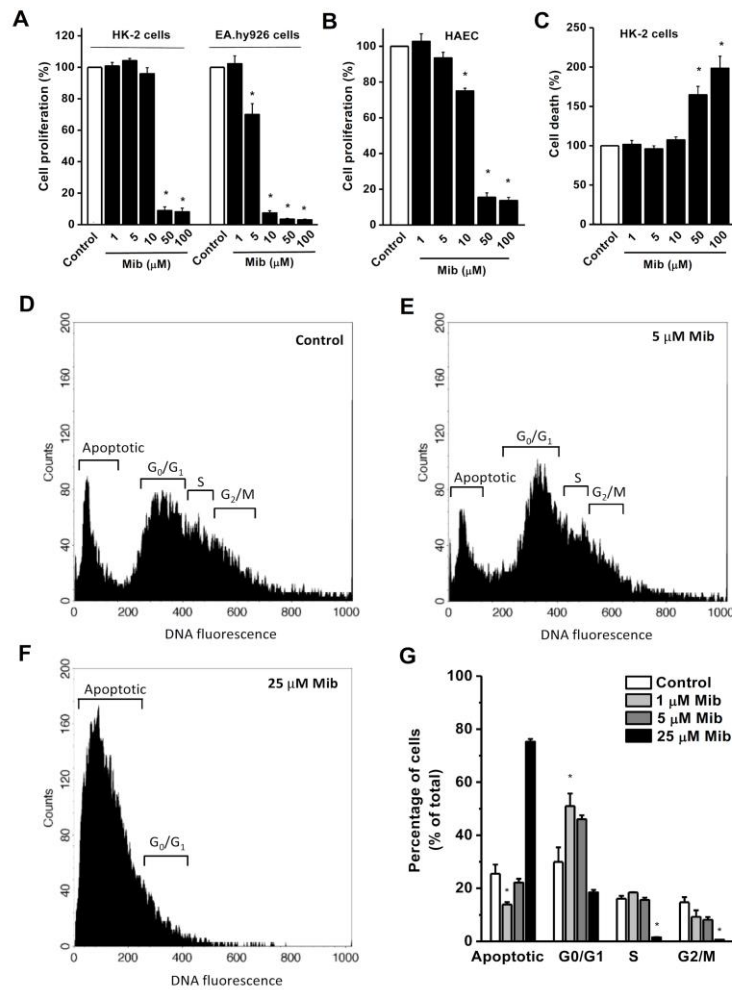
Figure 7 Effect of Mib on cell proliferation and cell death. The cell proliferation was monitored by WST-1 assay and the absorbance was measured at a wavelength of 450 nm with a reference at 650 nm. (A) Effect of Mib on the cell proliferation of HK-2 cells and EA.hy926 cells ($n = 8$ for each group). (B) Effect on human aortic endothelial cells (HAEC) ($n = 8$). (C) HK-2 cell death was detected by lactate dehydrogenase (LDH) release assay ($n = 8$). (D-F) Effect of Mib on cell cycle. Cells were stained with propidium iodide and the percentage of propidium iodide -labelled cells at different cell cycle stage was determined by FACS analysis. The representative FACS histogram for vehicle (D, Control) and Mib (5, 25 μM) for (E-F). (G) Mean ± SEM data from independent experiments ($n = 6$). * $P<0.05$ comparing with the control group.